Copolymer Microgels from Mono- and Disubstituted Acrylamides: Phase Behavior and Hydrogen Bonds

Martina Keerl,[†] Vytautas Smirnovas,[‡] Roland Winter,[‡] and Walter Richtering*,[†]

Physical Chemistry, RWTH Aachen University, Landoltweg 2, D-52056 Aachen, Germany, and Department of Chemistry, Physical Chemistry I, Dortmund University of Technology, Otto-Hahn-Str. 6, D-44227 Dortmund, Germany

Received April 9, 2008; Revised Manuscript Received June 30, 2008

ABSTRACT: The influence of microgel morphology and monomer substitution pattern of different copolymers on their phase transition is demonstrated by temperature-dependent light scattering, Fourier transform infrared spectroscopy, and small-angle neutron scattering. The data clearly illustrate that the ability of the neighbored side chains to form intramolecular hydrogen bonds and the flexibility of the backbone influence the phase transition temperature significantly. Copolymer microgels consisting of *N*-isopropylacrylamide (NIPAM) and *N,N*-diethylacrylamide (DEAAM) or *N*-isopropylmethacrylamide and DEAAM show a nonlinear dependence of the phase transition temperature on composition due to favored hydrogen bonds between DEAAM and the monosubstituted acrylamide. In the case of DEAAM−NIPAM copolymers this leads to a depression of the transition temperature below that of the homopolymers. Different microgel architectures, namely core−shell systems and random copolymer microgels, demonstrate the relevance of the local distribution of the monomer units inside the particle on the location of the phase transition.

Introduction

Synthetic polymers displaying temperature-induced phase transitions may be used as model systems for denaturation and folding processes of proteins. Synthetic polymers with a phase transition temperature at 30−40 °C have attracted particular attention.[1−3]

For example, aqueous solutions of poly-*N*-isopropylacrylamide (PNIPAM) undergo a reversible phase transition at 32 °C, which is attributed to the formation of intra- and intermolecular hydrogen bonds. The similarity of solution properties of PNIPAM and poly-*N*-isopropylmethacrylamide (PNIPMAM) polymers with protein folding processes has been pointed out previously.[4]

The phase transition temperature of PNIPAM was investigated by different methods like turbidity,[5] light scattering,[6] calorimetry,[7] fluorescence,[8] and infrared spectroscopy.[9,10] The transition is ascribed to a change in the intra- and intermolecular hydrogen bonding and therefore to a change in the solvent quality. PNIPAM with its amide groups as side chains is well-known to form strong hydrogen bond interactions and that these hydrogen bonds vary with the internal conformation of the chain.[11] The influence of the hydrogen bonding among the amide groups on the transition of a temperature-sensitive synthetic polymer was investigated by Fourier transform infrared spectroscopy (FTIR) measurements and density functional theory calculations.[12]

Linear temperature sensitive polymers are soluble at low temperatures but become insoluble as the temperature is increased above the lower critical solution temperature (LCST); a coil-to globule transition takes place. These linear polymers can be cross-linked, resulting in a temperature-sensitive gel network. The gel starts to shrink as the temperature is increased by expelling water over a narrow temperature range, usually called the volume phase transition temperature (VPTT).[13]

It is known that the phase transition of PNIPAM can be controlled by copolymerization with monomers having varying degrees of hydrophilicity/hydrophobicity,[14] by chemical cross-linking[15] or by a modification of the architecture, e.g., the core−shell structure.[16−20]The polymer chains become dehydrated upon the phase transition, and attractive interactions between hydrophobic moieties induce the change of the polymer conformation from a randomly coiled to a collapsed structure. Different hydrogen bond interactions can be distinguished in a cross-linked microgel. As a consequence, in a core−shell system, the intra- and intermolecular hydrogen bonds inside the core and in the shell determine the thermosensitive phase transition of the core and shell material. The core−shell interface exhibits additional hydrogen bond interactions between the core and the shell monomers.[21,22]

It is possible to probe such hydrogen bond interaction patterns in a core−shell system or a copolymer consisting of the same monomers by FTIR measurements. Recently, we investigated microgels with different architectures, namely core−shell and random copolymers by temperature-dependent FTIR spectroscopy, and we could show that the intra- and intermolecular hydrogen-bonding pattern is correlated with the microgel architecture.[21]

In this work, we investigated and compared microgel systems consisting of differently substituted acrylamides as depicted in Scheme 1. We prepared a copolymer microgel series of two temperature-sensitive acrylamides: NIPAM and *N,N*-diethylacrylamide (DEAAM) (copolymer 1). Poly-*N,N*-diethylacrylamide (PDEAAM) shows a broad phase transition temperature range of 26−32 °C,[23,24] i.e., a slightly lower VPTT as compared to PNIPAM. The copolymerization of the monosubstituted NIPAM and the disubstituted DEAAM leads to an unusual phase transition. The transition temperature of the DEAAM−NIPAM copolymer is suppressed *below* the phase transition temperature of the corresponding homopolymers PNIPAM and PDEAAM. This was explained by favored interactions of the polymer segments during the phase transition.[23] Different architectures lead to different transition temperatures; a PDEAAM core−PNIPAM shell system was investigated by means of light scattering and FTIR spectroscopy, but no suppression of the VPTT of the core−shell system in contrast to the copolymer

* Corresponding author: Ph +492418094670; Fax +492418092327; e-mail richtering@rwth-aachen.de.
[†] RWTH Aachen University.
[‡] Dortmund University of Technology.

10.1021/ma800785w CCC: $40.75
Published on Web 08/29/2008

Scheme 1. Schematic Drawing of the Different Microgel Types, the Copolymer Microgel with NIPAM and DEAAM (left), NIPMAM and DEAAM (middle), and a Core−Shell System (right)[a]

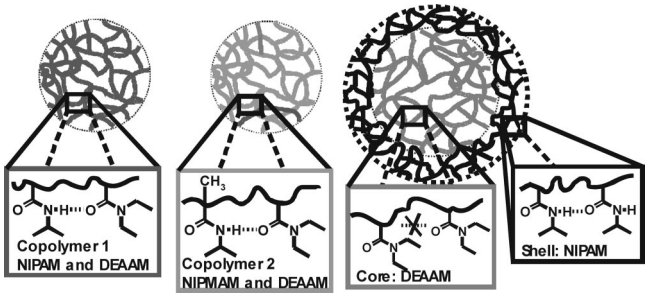

[a] Intramolecular hydrogen bonds between amide functionalities are shown in this scheme as well.

system was observed. The PDEAAM−PNIPAM core−shell microgel shows a phase transition temperature of 27 °C, i.e., is slightly shifted compared to the VPTT of the homopolymer PDEAAM.

The importance of a close neighborhood between the comonomers for the hydrogen bonds was demonstrated by comparing different architectures, namely core−shell systems and copolymers.[21] In this work we will explore the architecture of DEAAM−NIPAM microgels with SANS experiments and the influence of the increasing temperature on the alkyl part by a detailed discussion of the CH vibrational region.[25−27]

In addition to a copolymer consisting of DEAAM and NIPAM, a series of copolymer microgels with different amounts of disubstituted acrylamide DEAAM and monosubstituted acrylamide NIPMAM were prepared (Scheme 1), and the temperature-induced phase transition was determined with light scattering measurements. The homopolymer PNIPMAM shows a phase transition temperature of 42 °C, indicating that the additional α-methyl group in the backbone of the monosubstituted compound influences the phase transition temperature significantly.

We will show that the phase transitions of microgels consisting of mono- and disubstituted acrylamides depends strongly on the morphology and on the substitution pattern of the N-substituted acrylamides.

Experimental Part

N-Isopropylmethacrylamide (NIPMAM, Aldrich), *N*-isopropylacrylamide (NIPAM, Acros Organics), *N,N*-diethylacrylamide (DEAAM, Polyscience Inc.), sodium dodecyl sulfate (SDS, Fluka), potassium peroxodisulfate (KPS, Merck KGA), and cross-linker *N,N′*-methylenebis(acrylamide) (BIS, Merck KGA) were used as received. Water for all purposes was doubly distilled Milli-Q water.

The cross-linked copolymer microgels were synthesized via free radical dispersion polymerization as described previously.[23] In brief, the synthesis was performed in a 250 mL vessel equipped with a mechanical stirrer, thermometer, a reflux condenser, and a nitrogen inlet. The two monomers (NIPAM and DEAAM or NIPMAM and DEAAM; for details see Table 1), BIS, and SDS were dissolved in 150 mL of water at 75 °C and purged with nitrogen at least for 1 h. Polymerization was initiated by adding KPS (dissolved in 10 mL of degassed water at room temperature) and added to the monomer mixture. Polymerization was carried out for 6 h at 75 °C, a constant gas stream, and constant stirring of 330 rpm. The reaction mixture was allowed to reach room temperature under stirring overnight. The dispersion was filtered through glass wool and was purified three times by repeated ultracentrifugation (30 min, 50 000 rpm) and decantation of the supernatant and was redispersed in doubly distilled water. A Sorvall Discovery 90SE ultracentrifuge with a T865 rotor was used for the centrifugation at 20 °C.

The sample composition is indicated in the sample name, for example, PDEAAM−PNIPMAM(90/10) (copolymer 2, Scheme 1), where the first number denotes the mole percentage of the DEAAM monomer and the second number gives the percentage of NIPMAM in the monomer feed. It was not possible to determine the exact composition with NMR spectroscopy due to overlapping peaks; the numbers indicate the mole percentages that were used for the synthesis. The copolymer system of DEAAM and NIPAM is abbreviated PD-(55/45) (copolymer 1, Scheme 1), where the numbers indicates the sample composition. The sample composition of the PDEAAM−PNIPAM copolymer system was investigated by NMR spectroscopy.

Dynamic light scattering measurements were performed with an ALV goniometer and a laser light wavelength of 633 nm. The samples were highly diluted in H_2O ($c < 0.01$ wt %) to prevent multiple scattering and filtered through a 0.8 μm filter to remove dust. The scattered light was detected at a scattering angle of 40°, and hydrodynamic radius, $R_H(T)$, has been calculated from second-order cumulant fits via the Stokes−Einstein equation. Heating and subsequent cooling cycles have been performed. The particle size change is fully reversible. The VPTT of different microgel systems was determined as the inflection point of the temperature-dependent light scattering curve.

For the FTIR measurements, CaF_2 transmission windows and 0.05 mm Mylar spacers were used. The temperature in the cell was controlled through an external water circuit. All FTIR spectra were collected on a Nicolet 5700 FT-IR spectrometer equipped with a liquid nitrogen-cooled MCT detector. For each spectrum, 256 interferograms of 2 cm^{-1} resolution were co-added. The sample chamber was continuously purged with dry air. From the spectrum of each sample, a corresponding D_2O spectrum was subtracted. All the spectra were baseline-corrected and normalized. All data processing was performed with GRAMS software. FTIR measurements were carried out over a temperature range of 10−50 °C with a temperature increment of 2 K and with D_2O as solvent. The samples were investigated at mass concentration of 0.5 wt % in D_2O. To analyze the CH stretching region, a concentration of 2 wt % was used.[28]

SANS experiments were performed at the D11 beamline at the Institut Laue-Langevin (ILL) in Grenoble, France. A neutron wavelength with 6 Å was used. The data were collected on a ^{3}He detector with 64 × 64 pixels of 10 × 10 mm^2 size. A broad q range was covered by three detector distances of 2.5, 10.0, and 36.7 m. The incoherent scattering of water at sample−detector distances of 2.5 and 10 m was used for absolute intensity calibration. The microgels were investigated at mass concentrations of

Table 1. Composition of the Copolymerization Batches of DEAAM and NIPMAM (Copolymer 2) and Composition of the DEAAM−NIPAM Copolymers (Copolymer 1) (See Ref 23)

sample name	DEAAM (g)	NIPMAM (g)	BIS (g)	SDS (g)	KPS/(g)	monomer composition (mol %)	VPTT (°C)
PDEAAM	2.45		0.07	0.02	0.12	100/0	26
PDEAAM−PNIPMAM(90/10)	1.37	0.15	0.09	0.06	0.08	90/10	26
PDEAAM−PNIPMAM(78/22)	1.16	0.34	0.09	0.06	0.07	77.6/22.4	27
PDEAAM−PNIPMAM(53/47)	0.80	0.70	0.09	0.06	0.07	53.3/46.7	30
PDEAAM−PNIPMAM(28/72)	0.41	1.05	0.09	0.06	0.07	28.1/71.9	35
PDEAAM−PNIPMAM(10/90)	0.16	1.45	0.09	0.06	0.08	10.1/89.9	41.5
PNIPMAM						0/100	42

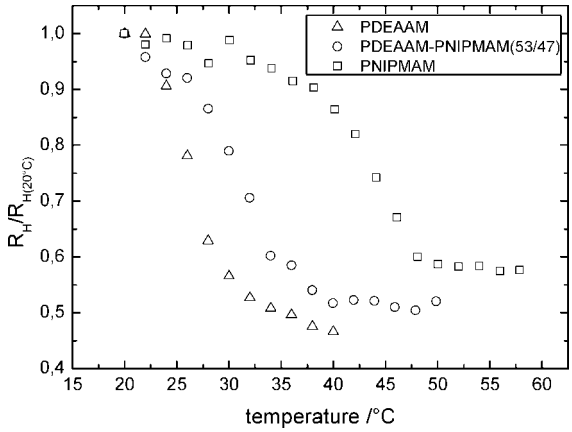

Figure 1. Temperature dependence behavior of the two homopolymers PDEAAM and PNIPMAM and the copolymer PDEAAM−PNIPMAM(53/47) (copolymer 2) in H_2O. All radii are normalized to the radius at 20 °C.

0.1 wt % in D_2O. The temperature was adjusted by an external thermostat.

Results and Discussion

The transition temperature of a temperature-sensitive nonionic copolymer can be controlled by different polarities and amounts of the comonomers.[29−31] The hydrophilicity or hydrophobicity of a monomer depends on its ability to build intra- and intermolecular hydrogen bonds. Acrylamides consist of different apolar regions like backbone and alkyl side chains; the polar behavior is dominated by the amide functional groups. The phase behavior of two different copolymer series with mono- and disubstituted thermosensitive acrylamides will be discussed in the next paragraph with focus on the composition dependence of the phase transition temperature.

Figure 1 shows the results of DLS experiments of the DEAAM−NIPMAM copolymer microgel series (copolymer 2). The hydrodynamic radius R_H (normalized to the radius in the swollen state at 20 °C) is plotted as a function of temperature. Three data sets are shown: the two homopoymers PNIPMAM and PDEAAM and the copolymer with 53 mol % of NIPMAM and 47 mol % of DEAAM. The VPTTs of the whole copolymer series can be found in Table 1.

Figure 1 demonstrates that the copolymer PDEAAM−PNIPMAM (copolymer 2) reveals a phase transition temperature of 30 °C, which lies in between the phase transition of the homopolymers PNIPMAM ($VPTT_{PNIPMAM}$ = 42 °C) and PDEAAM ($VPTT_{PDEAAM}$ = 26 °C). The transition temperatures of all copolymer microgels of this series are displayed in Figure 2. A nonlinear relationship between the copolymer composition and transition temperature can be observed. The comparison of the phase transition temperatures of the PDEAAM−PNIPMAM copolymer microgels (copolymer 2) with the previously reported copolymer system PDEAAM−PNIPAM (copolymer 1) clearly demonstrates that the phase transition temperatures of copolymers of mono- and disubstituted acrylamide monomers do not display a linear relationship between VPTT and composition.

As mentioned above, the VPTT depends on the balance of the hydrophilicity/hydrophobicity patterns of the comonomers as well as on the polar and unpolar regions. The influence of intra- and intermolecular hydrogen bonds on the phase transition temperature is directly related to the close neighborhood of the repeating units of NIPAM and DEAAM in the copolymer system and leads to a strong increase of the intramolecular (C═O···D−N−) hydrogen bond. Intermolecular hydrogen bonds (C═O···D−O−D) with the solvent D_2O are weakened

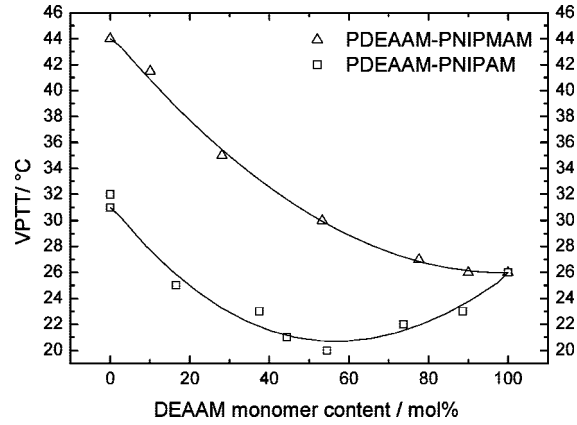

Figure 2. Influence of the composition on the phase transition temperature of two different copolymer microgel series: triangles, PDEAAM−PNIPMAM copolymer microgels (copolymer 2); squares, PDEAAM−PNIPMAM copolymer microgels (copolymer 1). Lines are used as guides for the eyes.

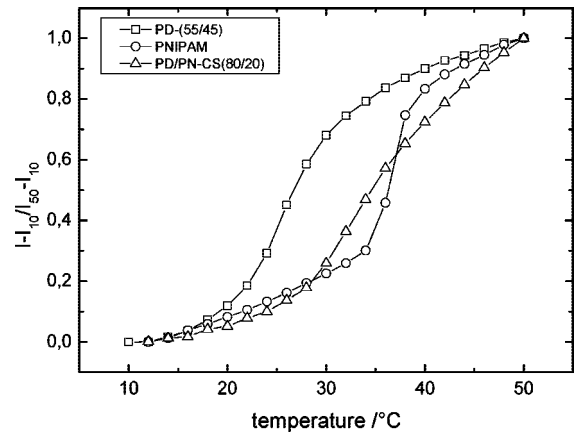

Figure 3. Temperature dependence of intramolecular components of the amide I′ band (peaks normalized to the intensity of the wavenumber at 1643 cm^{-1} at 50 °C) for PNIPAM, PD-(55/45) (copolymer 1), and a core−shell system (PD/PN-CS(80/20)).

with increasing temperature. This was shown recently by analyzing the amide I′ band in the FTIR spectrum.[21]

The comparison of the intensity of the amide I′ band at 1643 cm^{-1} of the two homopolymers and the copolymer PD-(55/45) shows that the increase of the intramolecular hydrogen bonds of the PD-(55/45) takes place at lower temperatures as compared to homopolymers (Figure 3).[21] This strong increase of the intramolecular hydrogen bonds of the PD-(55/45) copolymer microgel is favored by the −C═O···D−N− interaction of the neighboring monomer units. The intramolecular hydrogen bonds pattern of a PDEAAM core−PNIPAM shell microgel is shown in Figure 3 as well. The strong increase of the intramolecular hydrogen bonds takes place at nearly the same temperature as observed for the PNIPAM homopolymer system and can be related to the local separation of the different monomers in a core and shell region. The small shift of the increase in intensity is caused by the interface between core and shell where the monomer units are in a direct neighborhood.

Figure 4 shows examples of infrared absorption spectra of a microgel. The CH stretching region (3000 −2800 cm^{-1}) contains information about the hydration state of the alkyl groups of the polymers, the analysis of the amide I′ band (∼1600 cm^{-1}) provides information about the intra- and intermolecular hydrogen bonds, the amide II′ region (∼1500 cm^{-1}) is essentially determined by CN stretching vibrations, and at wavenumbers of ∼1300 cm^{-1} CH deformation bands can be found.[28]

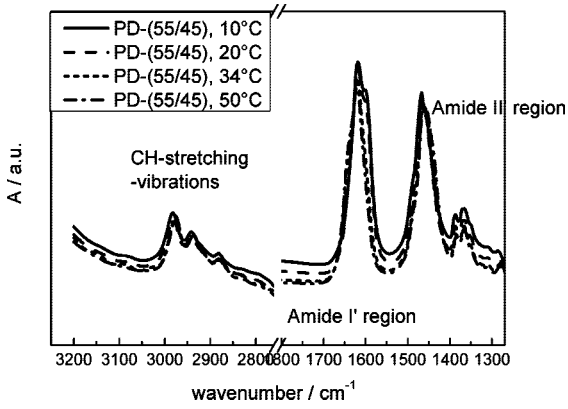

Figure 4. FTIR absorption spectra (3200−1250 cm^{-1}) of the PD-(55/45) copolymer microgel in D_2O at different temperatures.

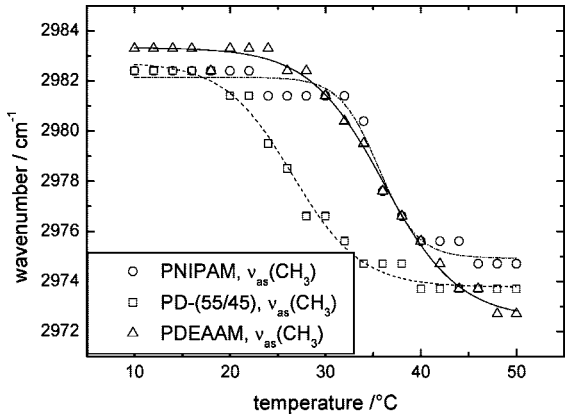

Figure 5. Temperature dependence of the shift of the antisymmetric CH stretching for $-CH_3$ for the two homopolymers PDEAAM and PNIPAM microgels and the copolymer PD-(55/45) (copolymer 1). Lines are used as guides for the eyes.

In our previous work we focused on the hydration state of the C═O groups. Here we will follow the dehydration of the polymer chains at high temperatures by analysis of the CH stretching region. In general, the IR bands of the CH_3 stretching vibrations undergo red shifts upon the phase transition, indicating dehydration of the alkyl groups.[32]

Figure 5 shows the temperature-dependent shift of the antisymmetric CH_3 stretching band of the alkyl side chains for three different systems: the two homopolymers PNIPAM and PDEAAM and the copolymer PD-(55/45) (copolymer 1). The interactions of the different polar and apolar regions in the monomer units with the neighboring water molecules are also reflected in the wavenumber of the CH_3 stretching vibration as reported for linear PDEAAM[28] and PNIPAM,[32,33] respectively.

The dehydration of the alkyl chain of the copolymer microgel takes place at a lower temperature as compared to the two homopolymer microgels. This is in good agreement with the previous analysis of using the hydration sensitivity of the C═O band vibration of these microgels.

So far, we have shown that the phase behavior is influenced by the different polar and apolar regions of the microgels, but also the architecture of a microgel is known to influence the phase transition.[16,34] An increasing shell thickness in PNIPAM core−PNIPMAM shell microgels changes the phase behavior markedly. A core−shell system with a thin shell shows a two-step phase transition in contrast to a core−shell microgel with a thick shell, where the swelling of the core is restricted by the shell, and therefore a one-step phase transition is observed. A chemomechanical model for doubly thermosensitive core−shell microgels has been explored by differential scanning calorimetry

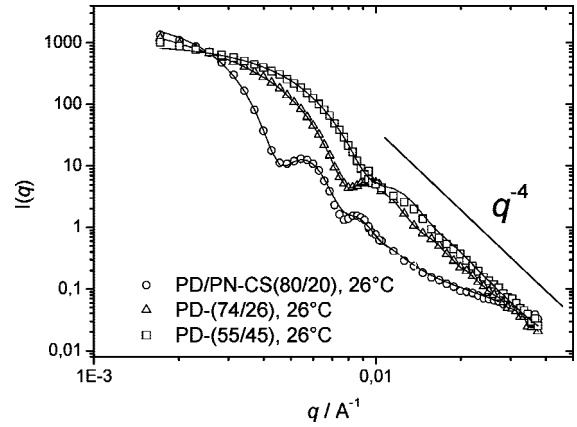

Figure 6. SANS profiles of PD-(55/45), PD-(74/26) (copolymer 1), and PD/PN-CS(80/20) (core−shell) at 26 °C. Both copolymers are in the collapsed state in contrast to the core−shell system.

(DSC) and by comparison of these results with a previously established form factor model of core−shell systems.[22] Core and shell regions with their individual thermosensitivity are directly chemically connected at the core−shell interface. The balance between the thermodynamic forces developed in the core material upon heating and the volume change of the shell leads to a stretching of the chain segments in the core−shell interface, and this competition between the thermodynamics and elastic forces results in unique properties of such core−shell materials.

Figure 3 shows that intramolecular hydrogen bonds in microgels are influenced by different microgel morphologies. To investigate the influence of the microgel architecture on the phase transition of PDEAAM−PNIPAM microgels, small-angle neutron scattering (SANS) measurements were performed. The experimental curve of the scattering intensity $I(q)$ as a function of the scattering vector q at $T = 26$ °C is depicted in Figure 6 (see Supporting Information Figures S2, S3, and S4 as well). The experimental data were fitted with well-established form factor models for PNIPAM microgels and PNIPAM−PNIPMAM core−shell systems.[35,36]

Two different architectures and *three* different compositions of microgels with DEAAM and NIPAM monomer units will be discussed in the following: *one* core shell system (PD/PN-(80/20)) and *two* copolymers, one with nearly the same composition as the core−shell system, PD-(74/26), and the other with a nearly equimolar composition of DEAAM and NIPAM, PD-(55/45). The VPTTs of these microgels were determined by light scattering measurements in D_2O: $VPTT_{(PD\text{-}(55/45))} = 20$ °C, $VPTT_{(PD\text{-}(74/26))} = 22$ °C (Figure 2), $VPTT_{(PD/PN\text{-}(80/20))} = 27$ °C.

The copolymer and the core−shell system with nearly the same molar ratio of DEAAM and NIPAM monomers show a different transition temperature due to the different architecture. The scattering profile of the copolymer PD-(74/26) in Figure 6 shows Porod scattering (i.e., $I(q) \sim q^{-4}$) at 26 °C, which is typical for a sharp surface in the fully collapsed state of a microgel. The scattering profile at 26 °C of the core−shell system PD/PN-(80/20), however, shows no Porod scattering. The PDEAAM core starts to shrink at 26 °C, but the PNIPAM shell ($VPTT_{(PNIPAM)} = 32$ °C) is still in the swollen state as indicated by the smaller slope at high q values (0.01−0.03 $Å^{-1}$). At 38 °C, both regions of the core−shell system are fully collapsed; hence, the intensity is proportional to q^{-4}, characteristic of a sharp surface (see Supporting Information, Figure S2).The copolymer PD-(55/45) with a nearly equimolar composition of DEAAM and NIPAM units is at 26 °C in the fully collapsed state like the copolymer PD-(74/26), and Porod scattering is observed as well.

Table 2. Assignment and Frequencies of Intra- and Intermolecular Hydrogen Bonds in the Amide I′ Region in D_2O of the Two Homopolymers PNIPMAM and PDEAAM and the Copolymer PDEAAM−PNIPMAM(53/47) (Copolymer 2)

sample	wavenumber (10 °C)/cm^{-1}	wavenumber (50 °C)/cm^{-1}	assignment
PNIPMAM	1633	1633	intramolecular C═O···D−N
	1606	1606	intermolecular C═O···D−O−D
PDEAAM		1637	"free" C═O
	1619	1620	weakly hydrated intermolecular C═O···D−N(D−O−D)
	1597	1598	strongly hydrated intermolecular C═O···D−O−D
PDEAAM−PNIPMAM (53/47)		1637(broad)	free C═O (or weak intramolecular)
	1620	1620	weakly hydrated intermolecular C═O···D−O−D
	1598	1598	intermolecular C═O···D−O−D

The comparison of the copolymer PD-(74/26) and the core−shell system PD/PN-(80/20) demonstrates that not only the composition plays an important role for the phase behavior but also the local distribution in different compartments such as core and shell regions. The copolymers exhibit a homogeneous structure with a statistical distribution of the two monomer units, whereas the core−shell microgel is characterized by spatially separated PNIPAM and PDEAAM regions.

However, not only the microgel architecture affects the phase transition. It is influenced by the acrylamide backbone as well as will be discussed for the PDEAAM−PNIPMAM copolymer microgel. The additional α-methyl group of the NIPMAM backbone governs the flexibility of the whole polymer chain, and more energy is required to compensate for this stiffness at the phase transition.[37] We focus on the amide I′ region of the PDEAAM−PNIPMAM(53/47) (copolymer 2) and compare the intra- and intermolecular hydrogen-bond interactions with the two homopolymer systems. A full spectrum of the copolymer microgel can be found in the Supporting Information (Figure S1). An analysis of the CH vibration region is not possible in this case due to overlapping asymmetric stretching vibrations of the α-methyl group in the backbone and the isopropyl side group of the NIPMAM unit.

Two main peaks in the FTIR spectrum of the PDEAAM homopolymer can be found, at 1620 and 1597 cm^{-1} (see Supporting Information, Figure S5).[28,38] The peak at 1620 cm^{-1} is assigned to a more hydrophobic environment of the C═O groups, and the peak at 1597 cm^{-1} is related to intermolecular hydrogen bonds to water. The FTIR spectrum of the homopolymer PNIPMAM shows two main peaks, at 1633 cm^{-1} (intramolecular H-bond) and at 1606 cm^{-1} (intermolecular H-bond).[33] Assignments and frequencies of intra- and intermolecular hydrogen bonds for the two homopolymers and the copolymer are listed in Table 2.

Figure 7 shows the FTIR spectrum of the copolymer microgel PDEAAM−PNIPMAM(53/47) (copolymer 2) at different temperatures. Two main peaks can be observed: the first one at 1620 cm^{-1} and the second at 1597 cm^{-1}. A broad shoulder

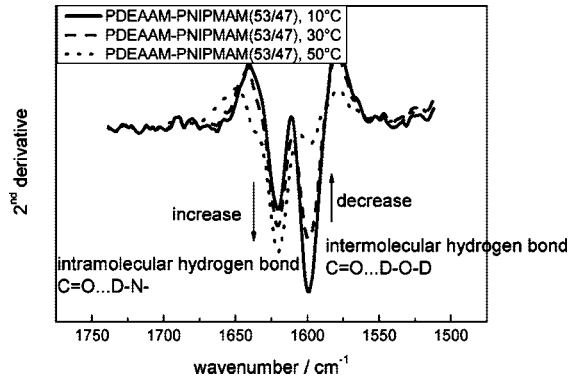

Figure 7. Second derivative of the amide I′ band of the copolymer microgel PDEAAM−PNIPMAM(53/47) (copolymer 2) in D_2O in the swollen state (10 °C), in the phase transition region (30 °C), and in the collapsed state (50 °C).

appears at 1637 cm^{-1} above the phase transition temperature ($VPTT_{(PDEAAM-PNIPMAM(53/47))}$ = 30 °C). The band at 1597 cm^{-1} decreases with increasing temperature. This indicates that this peak is related to intermolecular C═O stretching vibrations. The C═O stretching bands of the intermolecular hydrogen bonds of the two homopolymers show nearly the same positions, so it is difficult to distinguish if the peak at 1597 cm^{-1} of the copolymer microgel consists of a single C═O vibration related to DEAAM units or if it includes an additional contribution from the NIPMAM units. The peak at 1620 cm^{-1} increases with increasing temperature. The position of the weakly hydrated intermolecular hydrogen bond of the homopolymer PDEAAM is in good agreement with the wavenumber observed for the PDEAAM−PNIPMAM(53/47) copolymer (copolymer 2, Table 2). This peak can be related to a more hydrophobic environment of the C═O groups caused by the PDEAAM compound in the copolymer system. This peak broadens with increasing temperature due to contributions of the intramolecular C═O bond of NIPMAM. The shoulder at 1637 cm^{-1} is either related to vibrations of free C═O groups of DEAAM or intramolecular hydrogen bonds of the NIPMAM compound.

Figure 8a shows the temperature-dependent intensity of the intramolecular components of the amide I′ bands of PNIPMAM and the copolymer PDEAAM−PNIPMAM(53/47) (copolymer 2). The shape of the curves looks rather similar. The formation of the intramolecular hydrogen bonds of the copolymer microgel is shifted toward lower temperature compared to the PNIPMAM homopolymer. The increased intensity at frequencies related to vibrations of C═O···D−N(D−O−D) hydrogen bonds at low temperature indicates a favored polymer−polymer interaction between the DEAAM and NIPMAM monomer units. The temperature shift is in good agreement with the shifted temperature of the phase transition as observed by light scattering experiments (see Figure 1).

The temperature dependence of the intensity of the intermolecular components of the amide I′ band of the two homopolymers and the PDEAAM−PNIPMAM copolymer microgel system can be found in Figure 8b. The intensity of the homopolymer PDEAAM and the copolymer PDEAAM−PNIPMAM(53/47) (copolymer 2) intermolecular components of the amide I′ band decreases at the same temperature, but the shape of their curves is slightly different. The intensity decrease of the PDEAAM homopolymer intermolecular components of the amide I′ band takes place over a broader temperature range. The intermolecular C═O···D−O−D vibrations intensity of the PNIPMAM homopolymer microgel is reduced at a higher temperature compared with that of the copolymer system, indicating that the copolymerization of the DEAAM with the NIPMAM leads to a suppression of the hydrophilicity of the whole microgel. This suppressed hydrophilictiy is caused by the different substitution pattern of the monomers and their mutual interaction.

By comparing the two different copolymer systems PDEAAM−PNIPAM (copolymer 1) and PDEAAM−PNIPMAM (copolymer 2), the strong influence of the backbone on the phase transition is visible. Both copolymer series reveal a nonlinear

dependence of the monomer composition on the phase transition temperature (Figure 2), but only the PDEAAM−PNIPAM copolymer microgels show a strong suppression below the VPTT of the two corresponding homopolymers. The α-methyl group in the backbone of the PNIPMAM compound in the PDEAAM−PNIPMAM microgel (copolymer 2) restricts the free movement the polymer chain due to an additional stiffness and results in a higher phase transition temperature.

To highlight the influence of the substitution pattern of the side chains, we will compare our copolymer systems with well-established copolymer systems consisting of NIPAM and *N,N*-dimethylacrylamide (DMAAM). Soutar et al. studied the change in the balance of the hydrophilicity/hydrophobicity by a linear copolymer series of NIPAM and DMAAM.[39] They could show that an incorporation of DMAAM, which shows no temperature-dependent behavior in water, into the polymer structure raises the LCST of the copolymer system due to an increase of the hydrophilicity. Other groups reported the same temperature-dependent behavior; Shibayama et al. observed an increasing enthalpy change by thermal analysis of the copolymers and proposed that the second comonomer (DMAAM) affects the local environment of the NIPAM compound.[40] Benrebouh et al. synthesized different copolymers of *N*-alkylacrylamides as hydrogels and focused their attention on the relative hydrophilicity of the copolymers, hence the chemical structure and the composition of the constituent monomers.[30]

The solvation of PDMAAM and PDEAAM linear homopolymers in protic and aprotic solvents has been studied by infrared spectroscopy.[38] The comparison of the $\nu_{C=O}$ stretching mode frequencies of the two polymers in different solvents indicates that the PDEAAM is less solvated in a protic solvent due to steric hindrance of the side chains in contrast to the PDMAAM polymer. Not only the steric hindrance of the side chain influences the thermal behavior in aqueous and alcohol solutions; also, the tacticity of the tertiary acrylamide polymers plays an important role as could be shown by the analysis of the copolymer system of PDEAAM and PDMAAM.[41] The tacticity is dominated by the polymerization method (e.g., anionic: mainly isotactic structure, group transfer polymerization: syndiotactic) as reported for linear PDEAAM,[42] and this different spatial structure influences the phase transition temperature significantly (32−40 °C).[24,43]

To summarize, the main difference in the phase behavior of PDEAAM−PNIPAM (copolymer 1) and PDMAAM−PNIPAM copolymers is caused by the steric and solvation properties of the side chains. The ethyl group of the DEAAM monomer unit seems to have a favored orientation in a polymer chain in contrast to a DMAAM unit. Because of this favored orientation, formation of intramolecular hydrogen bonds is preferred between the NIPAM and DEAAM units and induces the strong suppression of the phase transition temperature observed. It is possible to apply this model of favored orientation of the ethyl side chains for the PDEAAM−PNIPMAM copolymer microgels as well. DEAAM monomer units have a preferred configuration in polymer segments. NIPAM and NIPMAM consist of the same isopropyl side chains; the only difference between the two monosubstituted acrylamides is the additional α-methyl group in the NIPMAM backbone which leads to a stiffer polymer chain. In contrast to the flexible NIPAM, the orientational dynamics of the NIPMAM monomer is hindered for steric reasons and restricts the whole copolymer system by rearrangement of intramolecular hydrogen bonds between the neighbored monomer units. The combination of the NIPMAM monomer with the DEAAM monomer leads to a nonlinear dependence between composition and phase transition temperature.

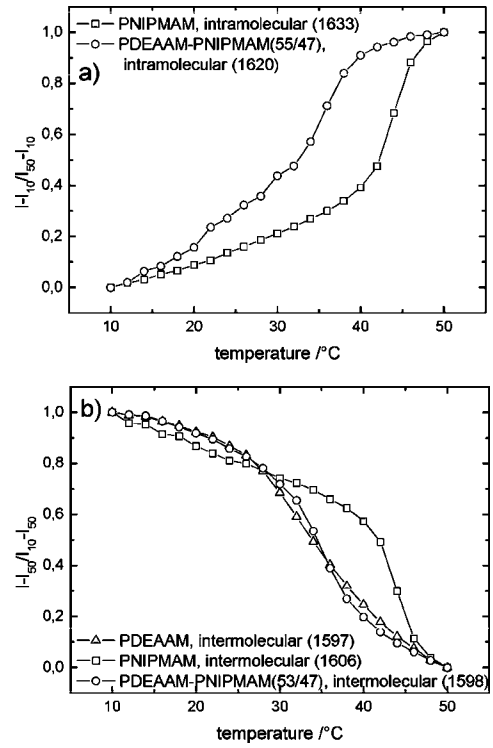

Figure 8. Temperature dependent intensity of (a) intramolecular components of the amide I′ band (normalized to the wavenumber at 1620 or 1633 cm^{-1}) of PNIPMAM and PDEAAM−PNIPMAM(53/47) (copolymer 2) and (b) intermolecular components of the amide I′ bands (normalized to the wavenumber at 1597 or 1606 cm^{-1}) for PDEAAM, PNIPMAM, and PDEAAM−PNIPMAM (53/47) copolymer.

Conclusions

The influence of the architecture and monomer substitution pattern on the phase transition temperature was demonstrated with thermosensitive polyacrylamides microgel systems consisting of DEAAM and NIPAM or DEAAM and NIPMAM, respectively, by means of temperature-dependent light and neutron scattering as well as FTIR spectroscopy measurements. The transition temperature of the copolymers depends on the composition, morphology and substitution pattern of monomers, and thus the ability to build intra- and intermolecular hydrogen bonds between the monomer units. Different regions can be distinguished in an acrylamide monomer: side chain, amide functionality, and backbone. The transition from the swollen to the collapsed state is correlated with the breaking of hydrogen bonds between polymer and water and the formation of intramolecular hydrogen bonds between monomer units. The favored hydrogen bonds between DEAAM and the monosubstituted monomer unit (NIPAM and NIPMAM, respectively) lower the VPTT, and thus a nonlinear relation between VPTT and composition is observed in both cases.

The influence of the modified backbone on the phase transition was shown by comparing two different copolymer microgel series: PDEAAM−PNIPAM and PDEAAM−PNIPMAM copolymers. The additional α-methyl group of the NIPMAM backbone restricts the flexibility of the entire copolymer system and thus hinders the formation of the intramolecular hydrogen bonds. Consequently, the VPTT of the NIPMAM-based microgels occurs at higher temperatures as compared to the NIPAM systems.

The influence of the local molecular interaction was investigated by different microgel architectures, namely core−shell and copolymer structures made of the two monomers DEAAM and NIPAM. Small-angle neutron scattering reveals the statisti-

cal distribution of DEAAM and NIPAM in the copolymer microgel in contrast to the local separation of shell and core region appearing in the core−shell system. In core−shell systems, the formation of hydrogen bonds is further determined by the spatial separation of the different monomer units. Thus, the combination of different monomers and microgel architectures employs aspects of supramolecular and colloid chemistry[44] and provides a toolbox for tailoring the properties of stimuli-sensitive microgels.

Acknowledgment. We gratefully acknowledge financial support by the Deutsche Forschungsgemeinschaft and the Fonds der Chemischen Industrie. We thank the ILL, Grenoble, France, for beam time at D11 and especially P. Linder for local support.

Supporting Information Available: Adsorption spectra of PDEAAM−PNIPMAM(53/47), SANS profiles of copolymers, and spectra of amide I′ band of PDEAAM and PNIPMAM. This material is available free of charge via the Internet at http://pubs.acs.org.

References and Notes

(1) Fujishige, S.; Kubota, K.; Ando, I. *J. Phys. Chem.* **1989**, *93*, 3311–3313.
(2) Lutz, J. F.; Akdemir, O.; Hoth, A. *J. Am. Chem. Soc.* **2006**, *128*, 13046–13047.
(3) Huber, S.; Jordan, R. *Colloid Polym. Sci.* **2008**, *286*, 395–402.
(4) Tiktopulo, E. I.; Uversky, V. N.; Lushchik, V. B.; Klenin, S. I.; Bychkova, V. E.; Ptitsyn, O. B. *Macromolecules* **1995**, *28*, 7519–7524.
(5) Heskins, M.; Guillet, J. E. *J. Macromol. Sci., Chem.* **1968**, *2*, 1441–1451.
(6) Wang, X. H.; Qiu, X. P.; Wu, C. *Macromolecules* **1998**, *31*, 2972–2976.
(7) Schild, H. G.; Tirrell, D. A. *J. Phys. Chem.* **1990**, *94*, 4352–4356.
(8) Winnik, F. M. *Macromolecules* **1990**, *23*, 233–242.
(9) Percot, A.; Zhu, X. X.; Lafleur, M. *J. Polym. Sci., Part B: Polym. Phys.* **2000**, *38*, 907–915.
(10) Maeda, Y.; Nakamura, T.; Ikeda, I. *Macromolecules* **2001**, *34*, 1391–1399.
(11) Scheiner, S. *J. Phys. Chem. B* **2007**, *111*, 11312–11317.
(12) Katsumoto, Y.; Tanaka, T.; Sato, H.; Ozaki, Y. *J. Phys. Chem. A* **2002**, *106*, 3429–3435.
(13) Pelton, R. *Adv. Colloid Interface Sci.* **2000**, *85*, 1–33.
(14) Feil, H.; Bae, Y. H.; Jan, F. J.; Kim, S. W. *Macromolecules* **1993**, *26*, 2496–2500.
(15) Senff, H.; Richtering, W. *Colloid Polym. Sci.* **2000**, *278*, 830–840.
(16) Berndt, I.; Richtering, W. *Macromolecules* **2003**, *36*, 8780–8785.
(17) Berndt, I.; Pedersen, J. S.; Richtering, W. *Angew. Chem., Int. Ed.* **2006**, *45*, 17371741; *Angew. Chem.* **2006**, *118*, 1769−1773.
(18) Nayak, S.; Lyon, L. A. *Angew. Chem., Int. Ed.* **2005**, *44*, 7686−7708; *Angew. Chem.* **2005**, *117*, 7862−7886.
(19) Blackburn, W. H.; Lyon, L. A. *Colloid Polym. Sci.* **2008**, *286*, 563–569.
(20) Singh, N.; Lyon, L. *Colloid Polym. Sci.* **2008**, *286*, 1061–1069.
(21) Keerl, M.; Smirnovas, V.; Winter, R.; Richtering, W. *Angew. Chem., Int. Ed.* **2008**, *47*, 338−341; *Angew. Chem.* **2008**, *120*, 344−347.
(22) Berndt, I.; Popescu, C.; Wortmann, F. J.; Richtering, W. *Angew. Chem., Int. Ed.* **2006**, *45*, 1081−1085; *Angew. Chem.* **2006**, *118*, 1099−1102.
(23) Keerl, M.; Richtering, W. *Colloid Polym. Sci.* **2007**, *285*, 471–474.
(24) Panayitou, M.; Pohner, C.; Vandevyver, C.; Wandrey, C.; Hilbrig, F.; Freitag, R. *React. Funct. Polym.* **2007**, *67*, 807–819.
(25) Herberhold, H.; Marchal, S.; Lange, R.; Scheyhing, C. H.; Vogel, R. F.; Winter, R. *J. Mol. Biol.* **2003**, *330*, 1153–1164.
(26) Zein, M.; Winter, R. *Phys. Chem. Chem. Phys.* **2000**, *2*, 4545–4551.
(27) Panick, G.; Malessa, R.; Winter, R.; Rapp, G.; Frye, K. J.; Royer, C. A. *J. Mol. Biol.* **1998**, *275*, 389–402.
(28) Maeda, Y.; Nakamura, T.; Ikeda, I. *Macromolecules* **2002**, *35*, 10172–10177.
(29) Mueller, K. F. *Polymer* **1992**, *33*, 3470–3476.
(30) Zhu, X. X.; Avoce, D.; Liu, H. Y.; Benrebouh, A. *Macromol. Symp.* **2004**, *207*, 187–191.
(31) Liu, H. Y.; Zhu, X. X. *Polymer* **1999**, *40*, 6985–6990.
(32) Schmidt, P.; Dybal, J.; Trchova, M. *Vib. Spectrosc.* **2006**, *42*, 278–283.
(33) Maeda, Y.; Nakamura, T.; Ikeda, I. *Macromolecules* **2001**, *34*, 8246–8251.
(34) Jones, C. D.; Lyon, L. A. *Macromolecules* **2000**, *33*, 8301–8306.
(35) Stieger, M.; Richtering, W.; Pedersen, J. S.; Lindner, P. *J. Chem. Phys.* **2004**, *120*, 6197–6206.
(36) Berndt, I.; Pedersen, J. S.; Lindner, P.; Richtering, W. *Langmuir* **2006**, *22*, 459–468.
(37) Tirumala, V. R.; Ilavsky, J.; Ilavsky, M. *J. Phys. Chem. B* **2006**, 124.
(38) Katsumoto, Y.; Tanaka, T.; Ozaki, Y. *J. Phys. Chem. B* **2005**, *109*, 20690–20696.
(39) Barker, I. C.; Cowie, J. M. G.; Huckerby, T. N.; Shaw, D. A.; Soutar, I.; Swanson, L. *Macromolecules* **2003**, *36*, 7765–7770.
(40) Shibayama, M.; Mizutani, S.; Nomura, S. *Macromolecules* **1996**, *29*, 2019–2024.
(41) Popkov, Y. M.; Nakhmanovich, B. I.; Chibirova, F. K.; Bune, E. V.; Arest-Yakubovich, A. A. *J. Polym. Sci., Ser. B* **2007**, *49*, 155–158.
(42) Freitag, R.; Baltes, T.; Eggert, M. *J. Polym. Sci., Part A: Polym. Chem.* **1994**, *32*, 3019–3030.
(43) Panayiotou, M.; Garret-Flaudy, F.; Freitag, R. *Polymer* **2004**, *45*, 3055–3061.
(44) Cohen Stuart, M. *Colloid Polym. Sci.* **2008**, *286*, 855–864.

MA800785W